Surgery 165 (2019) 345–352

Contents lists available at ScienceDirect

Surgery

journal homepage: www.elsevier.com/locate/surg

Hepatic regeneration by associating liver partition and portal vein ligation for staged hepatectomy (ALPPS) is feasible but attenuated in rat liver with thioacetamide-induced fibrosis ☆

Tong Yifan, PhD [a], Xu Ming, PhD [a], Wang Yifan, PhD [a], Ying Hanning, PhD [a], Jiang Guangyi, PhD [a], Yan Peijian, PhD [a], Wu Ke, PhD [a], Cai Xiujun, MD, FACS, FRCS [a,b,*]

[a] Department of General Surgery, Sir Run Run Shaw Hospital, School of Medicine, Zhejiang University, Hangzhou, China
[b] Zhejiang Provincial Key Laboratory of Laparoscopic Technology, Hangzhou, China

ARTICLE INFO

Article history:
Accepted 8 August 2018
Available online 22 September 2018

ABSTRACT

Background: The associating liver partition and portal vein ligation for staged hepatectomy (ALPPS) procedure promotes the proliferation of the future liver remnant, but evidence to support the feasibility of ALPPS in livers with fibrosis is needed. Therefore the aim of this study was to establish a fibrotic ALPPS model in the rat to compare the capacity of regeneration in the remnant liver with or without fibrosis.

Methods: In our study we first established a thioacetamide-induced fibrotic ALPPS model in rats. Then the ALPPS-induced regenerative capacities of normal and fibrotic liver were compared in this animal model. In addition, markers of regeneration, including the proliferative index and cyclin D1 and proliferating cell nuclear antigen levels, as well as various indicators of liver function were determined to evaluate the quality of the hepatic regeneration.

Results: Compared with that of the sham group (opening of the peritoneal cavity with no further operative manipulation), the proliferation of the future liver remnant in fibrotic rat liver after the ALPPS procedure was increased on postoperative days 1, 2, and 5 ($P < .039$ each). In addition, the proliferative response was greater in the ALPPS group than in the ligation group subjected only to portal vein ligation of the left lateral, left middle, right, and caudate lobes ($P = .099$, $P = .006$, and $P = .020$ on postoperative days 1, 2, and 5, respectively). In contrast, the ALPPS-induced regenerative capacity in the fibrotic rat livers was attenuated compared with that in the normal liver on postoperative days 1, 2, and 5 ($P < .031$ for each) after stage I and on postoperative day 5 after stage II of the ALPPS procedure ($P < .005$). This attenuated the recovery of liver function, and the greater mortality rate indicated that functional proliferation was either delayed or not as extensive in the fibrotic rat livers.

Conclusion: Through establishing a rat model of thioacetamide-induced liver fibrosis, we found that ALPPS-derived liver regeneration was present and feasible in fibrotic livers, but this effect was attenuated compared with that in normal liver.

Introduction

Despite newly developed therapies, such as transcatheter arterial chemoembolization, radiofrequency ablation, and sorafenib, liver resection remains the only potentially curative therapy for hepatic malignancies.[1,2] Posthepatectomy liver failure (PHLF) caused by the insufficient function of the future liver remnant (FLR) hinders more radical hepatectomies in several clinical settings.[3] Therefore the associating liver partition and portal vein ligation for staged hepatectomy (ALPPS) procedure has become increasingly popular worldwide.[3,4] During stage 1 of ALPPS, the branch of the portal vein to the part of the liver to be resected later during stage 2 of ALPPS, combined with transection of the parenchymal continuity between the liver to be removed and the FLR, accelerates the hypertrophy of the FLR. Then the second stage of ALPPS follows with the removal of the deportalized part of the liver, provided the FLR reaches an appropriate size and function after the removal of the deportalized liver to allow adequate liver function after this major hepatectomy. According to data from the ALPPS registry (www.alpps.net), severe complications

☆ This study was supported by the Public Welfare Technology Application Project of Zhejiang Province (Grant No. 2017C33043, Recipient: Wang Yifan).

* Corresponding author: Department of General Surgery, Sir Run Run Shaw Hospital, School of Medicine, Zhejiang University, Hangzhou, 310000, China.
E-mail addresses: srrsh_cxj@zju.edu.cn, cxj_srrsh@zju.edu.cn (C. Xiujun).

https://doi.org/10.1016/j.surg.2018.08.014
0039-6060/

(Clavien-Dindo grade ≥ IIIb) of 27% and a mortality rate of 9% for ALPPS have prompted the hepatobiliary community to re-evaluate its cost to benefit ratio.[5]

Liver fibrosis, a pathologic condition characterized by excessive, postdestructive regeneration of the hepatic parenchyma, is a precursor to cirrhosis and increases the chance of developing hepatocellular carcinoma.[6,7] As suggested by previous studies indicating that the partial hepatectomy–induced regenerative capacity is attenuated in livers with fibrosis, the feasibility of the ALPPS procedure has to be questioned in livers with fibrosis or cirrhosis.[6,7] Only a few studies with a limited number of cases have been reported where patients with fibrosis or cirrhosis have undergone an ALPPS procedure.[5,8,9] Until now, the evidence to support the feasibility of ALPPS in livers with fibrosis or cirrhosis has been scarce; several studies have used animal models of ALPPS, but these animals had a normal, nonfibrotic liver (Table 1).[10-23]

Prolonged exposure to thioacetamide (TAA), a potent hepatotoxin that causes necrosis around the central veins after acute administration, will result in bile duct proliferation and pathologic indicators of liver fibrosis or cirrhosis.[24] Therefore, the aim of this study was to establish a TAA-induced model of hepatic fibrosis in the rat to evaluate the feasibility of using ALPPS for fibrotic livers; we also compared the regenerative capacity in rat livers with or without fibrosis using several operative models. These findings will provide a theoretical foundation to improve the clinical safety and feasibility of the ALPPS procedure in patients with hepatic fibrosis and cirrhosis.

Methods

Animals and ethics

In this study we used male Sprague-Dawley rats, aged 8 to 10 weeks and weighing 200 to 250 g, from the Experimental Animal Center of Zhejiang Province, China. All rats were housed in a restricted access room with a controlled temperature (23°C) and light/dark (12 h/12 h) cycle; the rats had free access to food and water before and after treatment. The protocol was reviewed and approved by the Animal Ethics Committee of Zhejiang University, Hangzhou, China. In addition, all experiments were performed in accordance with the ARRIVE (Animal Research: Reporting In Vivo Experiments) guidelines, which are considered key for describing a study comprehensively and transparently.[25]

Study design

The entire study contained several steps as described later. Initially, thioacetamide (0.1 g/mL) was injected intraperitoneally twice a week (2.0 mL/kg) to establish the rat model of hepatic fibrosis. Based on the severity of fibrosis (using the Ishak score[26]) after different durations of TAA treatment, a reliable model of TAA-induced hepatic fibrosis was determined using 9 consecutive weeks of TAA treatment. Next we established the model for the ALPPS procedure in rats with normal livers. Then the rats were divided randomly into an ALPPS group, a ligation group, a partition group, and a sham group. We used only 3 experimental groups for rats with TAA-induced fibrotic livers: an ALPPS group subjected to the ALPPS procedure; a ligation group subjected to the ligation of the portal veins to the left lateral, left middle, right, and caudate lobes; and a sham group subjected only to the opening of the peritoneal cavity and closing the abdomen, because the FLR in the partition group did not lead to any relevant FLR hypertrophy in normal liver. In the ALPPS (A) group, the portal vein supplying the left lateral, right, and caudate lobes was ligated after the transection of the middle lobe parenchyma. In the ligation (L) group, only the portal vein supplying the left lateral, right, and caudate lobes was ligated. In

Table 1
Systemic review of ALPPS animal models

Year	Authors	Species	Future liver remnant	With PHx	Point-in-time after stage I	Proliferation (%)	Regenerative speed, percentage (day)
2014	Schlegel et al	Mouse	Left middle lobe	Yes	Day 1, 2, 7	300% at seventh day	43% ($n = 6$)
2014	Almau et al	Rat	Right middle lobe	No	Day 3, 7, 14	79% at seventh day	11% ($n = 10$)
2014	Yao et al	Rat	Right middle lobe	No	Day 1, 2, 3, 7	159% at seventh day	23% ($n = 6$)
2015	Croome et al	Pig	Partial right lobe + caudate lob	Yes	Day 7	76% at seventh day	11% ($n = 13$)
2015	Dhar et al	Rat	Right middle lobe	No	Day 1, 2, 4, 7	140% at seventh day	20% ($n = 6$)
2015	García-Pérez et al	Rat	Left middle lobe + caudate lobe	No	1 hDay 1, 2, 812 weeks	Not mentioned	Not mentioned ($n = 5$)
2015	Shi et al	Rat	Left middle lobe	Yes	Day 1, 2, 3, 7	241% at seventh day	34% ($n = 4$–6)
2016	Wei et al	Rat	Right middle lobe	No	Day 1, 2, 3, 7	135% at seventh day	19% ($n = 6$)
2016	Liao et al	Rabbit	Right middle lobe (different percentages of ligated lobes)	No	Day 3, 7	44% at seventh day	6% ($n = 5$)
2016	Linecker et al	Mouse	Left middle lobe (different levels of liver partition)	Yes	Day 1, 2	155% at second day	77% ($n = 5$)
2017	Langiewicz et al	Mouse	Left middle lobe	Yes	12 hDay 1, 2, 7	400% at seventh day	57% ($n = 6$)
2017	Andersen et al	Rat	Right middle lobe	No	Day 1, 2, 3, 4	29% at fourth day	7% ($n = 8$)
2017	Sheng et al	Rat	Right middle lobe	No	Day 7	170% at seventh day	24% ($n = 10$)
2017	Deal et al	Pig	Right lobe + caudate lobe	No	Day 7	64% at seventh day	9% ($n = 4$)

PHx, partial hepatectomy. Proliferation (%) = (Postoperative future liver remnant - Preoperative future liver remnant)/Preoperative future liver remnant * 100%; Regeneration speed (percentage/day) = Proliferation (%)/days.

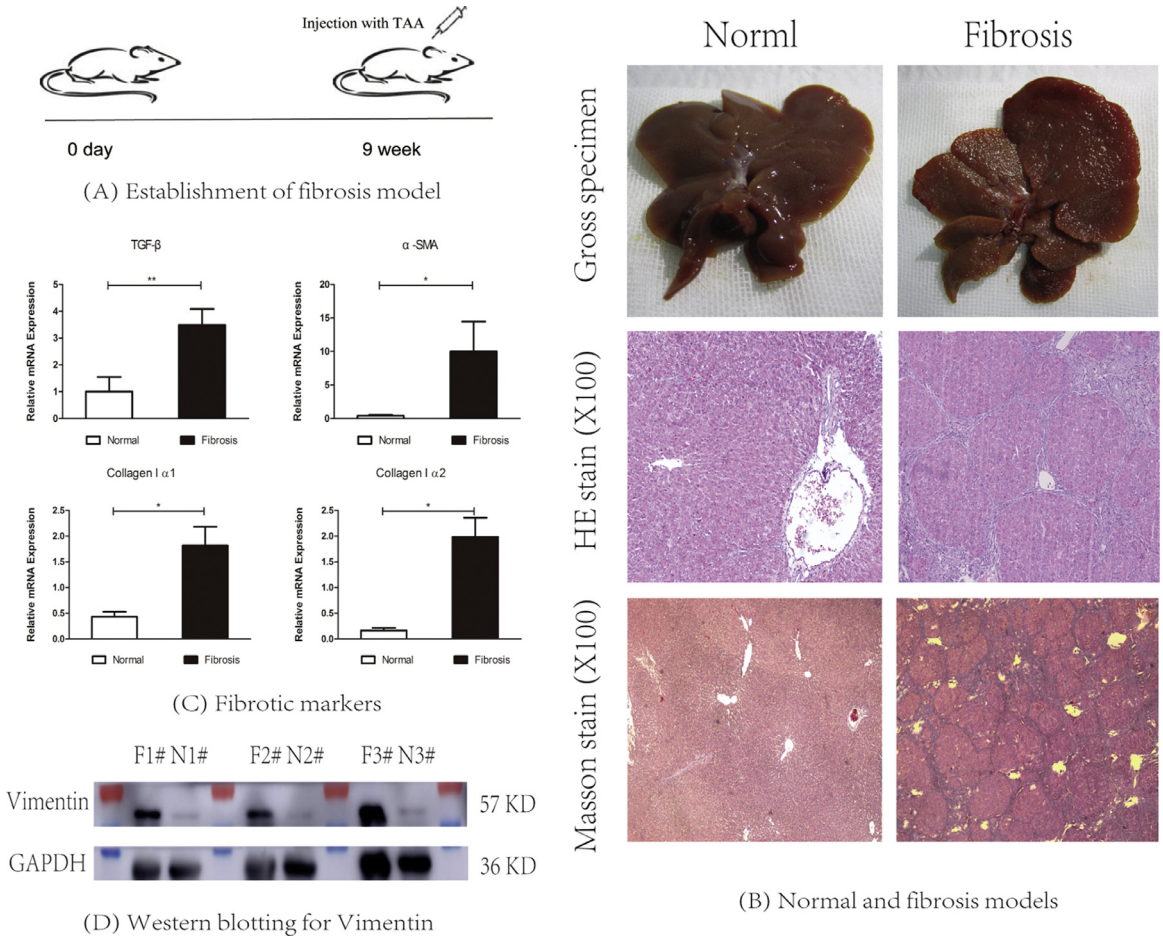

Fig. 1. Establishment of a TAA-induced fibrosis model. (A) TAA-induced fibrosis model (n=3 for each condition). (B) Specimens from normal and fibrotic livers; HE staining of normal and fibrotic livers (X100) and Masson staining of normal and fibrotic livers (X100) show the deposition of collagenous fibers and formation of pseudolobules. (C) Relative mRNA expression levels of TGF-β, α-SMA, collagen I α1 and collagen I α2 between normal and fibrotic livers. (D) Western blott analysis of vimentin in livers with or without fibrosis. TAA, thioacetamide; HE, hematoxylin-eosin.

the partition (P) group, only the middle lobe parenchyma was transected. In the sham (S) group, the peritoneal cavity was opened and closed. Each group contained 6 rats for each time point ($n=6$). Afterward, the capacity of ALPPS-derived liver regeneration in rats with normal livers and rats with TAA-induced fibrotic livers was compared.

Operative technique

All rats ($N=162$) were fasted for 8 hours before the operations. Under general anesthesia with 8% chloral hydrate (5.0 mL/kg) via intraperitoneal injection, the rats were subjected to a transverse abdominal incision. For the ALPPS procedure, in brief, after the left lateral lobe was dissected, the portal vein supplying the corresponding lobe was ligated with 5-0 silk. Artery and biliary duct branches were maintained. Then the same procedure was conducted for the portal branches of the right and caudate lobes. Along with the ischemic demarcation line of the middle lobe, the parenchyma was partitioned with bipolar energy at 40 Joules (*See* Fig 2 *B*). For stage II, the left lateral, left middle, right, and caudate lobes were removed on the fifth day after stage I of the ALPPS procedure. Given that the metabolism of rats is much faster than that of humans, the FLR proliferation is correspondingly accelerated. Therefore the rats were killed on day 0 for baseline measurements ($n=6$), as well as on days 1, 2, and 5 after the operation. Blood samples were obtained by cardiac puncture and were used to detect liver injury. After weighing, specimens were preserved and fixed in formaldehyde for subsequent analyses.

Proliferation of the FLR

Proliferation of the FLR was assessed by the right middle lobe (RML) weight-to-body weight (BW) ratio. To further confirm the regenerative response, proliferation markers, including Ki67, proliferating cell nuclear antigen (PCNA), and cyclin D1, were assessed. In addition, the proliferative index (PI), or the ratio of Ki67-positive hepatocytes, was calculated randomly in 4 visual fields ($\times$ 200) by Image-Pro Plus 5.1 (Media Cybernetics, Inc, Rockville, MD, USA) and was used for the quantitative analysis of proliferation.

Assessment of the liver injury

Biochemical analyses for alanine transaminase (ALT), albumin, total bilirubin, and prothrombin time (PT) were used for assessing liver injury. The serum levels of ALT, albumin, and total bilirubin were detected by an Abbott Architect c-system. The corresponding reagents were 7D56 ALT Reagent Kit (Abbott Diagnostics, Shanghai, China), 7D53 Albumin BCG (Abbott, China), and Total Bilirubin Kit (Abbott). A Coulter LH 750 automatic detection system (Beckman-Coulter, Inc, Fullerton, CA) was applied for detecting the PT. Measurement of P450 enzymes and inflammatory markers was conducted by quantitative real-time polymerase chain reaction (PCR) as described later.

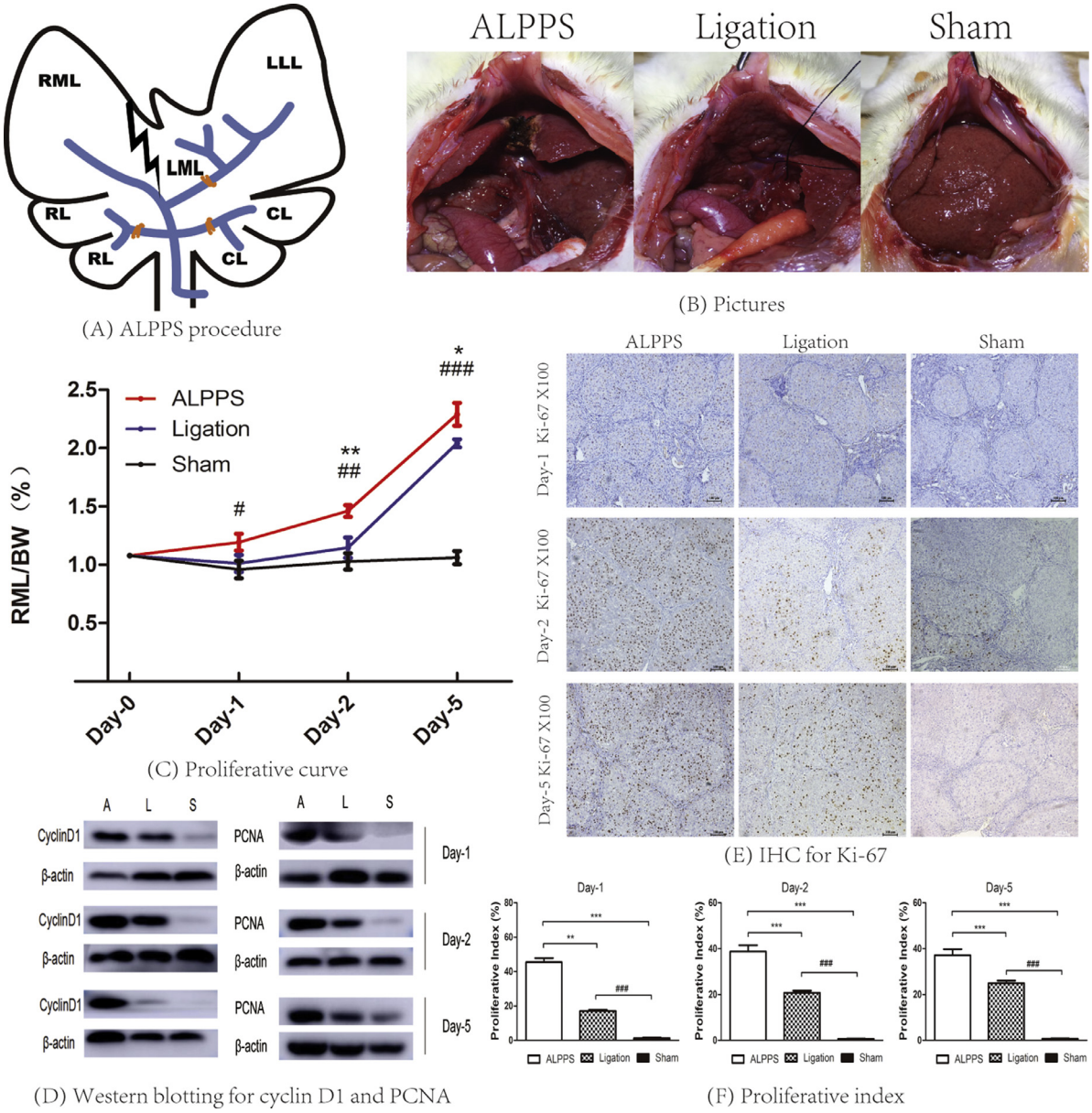

Fig. 2. ALPPS model in livers with fibrosis. (A) Schematic diagram of the ALPPS procedure. (B) Images of the ALPPS, ligation, and sham groups. (C) The proliferation curve in the fibrotic liver model (n=6 for each condition). * and # represent the ALPPS group and the ligation group compared with the other groups, respectively. *P<0.05, **P<0.01, ***P<0.001 and #P<0.05, ##P<0.01, ###P<0.001. (D) Western blot of PCNA and cyclin D1 for each group. (E) Representative images of Ki67 staining by IHC for each group (X200). (F) Proliferative index in the groups. TAA, thioacetamide; RML, right middle lobe; BW, body weight; HE, hematoxylin-eosin; IHC, immunohistochemistry.

Quantitative real-time PCR

Total RNA was extracted from 50 mg of liver specimens by TRIzol reagent (CWBio Co, Ltd, Beijing, China). Five micrograms of RNA was reverse-transcribed using the HiFiScript cDNA Synthesis Kit (CWBio) to yield the complementary DNA template. Quantitative, real-time PCR amplification was performed by a Roche Light Cycler 480II. The expression of messenger RNA is shown as the fold induction. The primers for interleukin-6, tumor necrosis factor α, transforming growth factor β (TGF-β), α smooth muscle actin, collagen I α1, and collagen I α2, as well as P450 enzymes, including CYP1A1, CYP2D6, and CYP3A1, are listed in Supplementary Table 1 (online version only).

Histologic examination

Liver tissues were immersion fixed in 4% formaldehyde, embedded, sectioned, gradient dehydrated, and stained with hematoxylin-eosin (HE) or subjected to immunohistochemistry. To verify TAA-induced fibrosis, Masson staining was performed with a Masson kit (Jiancheng Science and Technology Ltd, Nanjing, China).

Western blotting

Standard Western blotting assays were performed to analyze protein expression as described previously.[27] In brief, samples were treated with lysis buffer, and the proteins were separated on 10% to 12% sodium dodecyl sulfate polyacrylamide gels and then transferred onto polyvinylidene difluoride membranes (Millipore, Bedford, MA). After blocking, the membranes were incubated with the appropriate dilutions of specific primary antibodies overnight. The blots were incubated with horseradish peroxidase–conjugated secondary antibodies and visualized using an enhanced chemiluminescence system (ThermoFisher Scientific, Rochester, NY). The antibodies against Ki67 (ab15580), PCNA (ab29), cyclin D1 (ab134175), and β-actin (ab8226) were produced by Abcam

(Cambridge, MA), and vimentin (no. 5741) was obtained from Cell Signaling Technology (Beverly, MA).

Statistical analysis

Data are expressed as the mean with standard deviation or median with range and compared with Student's *t* test or Mann-Whitney *U* test. The differences between groups were assessed by 1-way analysis of variance (least significant difference post-test). Statistical analyses in this study were performed using SPSS Version 22.0 for Windows (IBM Corp, Armonk, NY).

Results

Establishment of the rat model of TAA-induced fibrosis

After consecutive drug treatment for 6, 9, and 12 weeks, the liver presented with varying degrees of fibrosis ($n = 3$ for each condition; Supplementary Fig 1). On the basis of the classic Ishak scoring system, a feasible fibrosis model with a granular nodular pathologic condition was determined after 9 weeks treatment with TAA (Fig 1 *A*). Furthermore, HE and Masson staining identified the deposition of collagenous fiber and the formation of pseudolobules (Fig 1 *B*). According to the increased expression levels of cytokines promoting the deposition of collagen fibers, including TGF-β, α smooth muscle actin, collagen I α1, and collagen I α2, and the increase in vimentin protein levels, the formation of TAA-induced fibrosis was further confirmed (Fig 1, *C* and *D*).

Establishment of an ALPPS model

For the ALPPS model in normal liver ($n = 6$), we ligated the portal vein to the right and caudate lobes and the common trunk of the left lateral and middle lobes. Then transection was performed between the left and right middle lobes (Supplementary Fig 2, *A*). Likewise, other models (ligation, partition, and sham models, $n = 6$ for each condition) were established successfully (Supplementary Fig 2, *A*). The regeneration of the FLR induced by the different operative procedures was compared (Supplementary Table 2). When compared with the baseline level (n=6) of RML/BW of 1.09% (1.01%–1.12%), the mean RML/BW ratio increased rapidly to 1.50% (1.28%–1.63%), 1.80% (1.54%–2.11%), and 2.97% (2.33%–4.42%) on day 1, day 2, and day 5, respectively, after stage I of the ALPPS procedure. The ratios of the ligation, partition, and sham groups (n=6 for each group) were 1.20% (0.87%–1.52%), 1.10% (0.95%–1.19%), and 1.14% (0.98%–1.40%) on the first day, 1.59% (1.50%–1.67%), 1.20% (0.93%–1.46%), and 1.16% (1.00%–1.25%) on the second day, and 2.46% (2.25%–2.78%), 1.44% (1.14%–2.14%), and 1.06% (0.87%–1.22%) on the fifth day ($n = 6$ rats per day; Supplementary Fig 2, *B*). As shown earlier, the ALPPS procedure induced a greater regenerative response, although there were no significant differences between the ALPPS and ligation groups on day 2 ($P = .059$) and day 5 ($P = .171$). To further investigate the regenerative response, detection of Ki67, PCNA, and cyclin D1 was performed; the upregulation of these markers indicated greater proliferative activity in the ALPPS group (Supplementary Fig 2, *C* and *D*). For quantitative analysis, the increased PI of the ALPPS group confirmed substantial liver regeneration (Supplementary Fig 2, *E,* and Supplementary Table 3).

The feasibility of ALPPS in rat liver with TAA-induced fibrosis

To investigate the feasibility of ALPPS in rat livers with fibrosis, the ALPPS, ligation and sham groups were studied ($n = 6$ for each condition; Fig 2 *B*). Regarding regeneration of the FLR, the mean RML/BW ratio was 1.08% (1.01%–1.15%) at baseline, and was similar to that of normal livers. On postoperative days 1, 2, and 5, the mean RML/BW ratios were 1.19% (0.92%–1.41%), 1.46% (1.32%–1.65%) and 2.29% (2.06%–2.65%), respectively, in the ALPPS group and 0.96% (0.65%–1.17%), 1.03% (0.85%–1.32%), and 1.06% (0.96%–1.33%) in the sham group (Supplementary Table 2). These results strongly indicated the dramatic induction of regenerative capacity by the ALPPS procedure ($P < .039$ at each time point). In addition, compared with that of the ALPPS group, the induced proliferation tended to be less in the ligation group (ALPPS versus ligation, 1.19% vs 1.01%, $P = .099$, on day 1; 1.46% vs 1.16%, $P = .006$, on day 2; 2.29% vs 2.04%, $P = .020$, on day 5; Fig 2, *C*). The expression levels of the proliferation-associated markers Ki67, PCNA, cyclin D1, and PI were also increased in the ALPPS group, suggesting an accelerated regenerative response compared with the other groups (Fig 2, *D, E,* and *F,* and Supplementary Table 3).

Comparison of ALPPS-derived liver regeneration in normal and fibrotic models

To further evaluate the feasibility of the ALPPS procedure in rat liver with fibrosis, a comparison of ALPPS in normal and fibrotic livers was conducted. With the same ALPPS procedure, the mean RML/BW ratios in livers with fibrosis ($n = 6$ for each condition) were significantly lower than those in normal livers, whereas no differences were found between the 2 sham groups (Fig 3, *A*). Furthermore, compared with the proliferation indices for ALPPS in livers with fibrosis, those for ALPPS in normal livers indicated a greater regenerative capacity (Fig 3, *B,* and Supplementary Table 3). Likewise, the greater expression of PCNA and cyclin D1 suggests that the regenerative response remained activated even on the fifth day after stage I of the ALPPS procedure in normal livers (Fig 3, *C*).

In terms of liver injury, the messenger RNA levels of interleukin-6 and tumor necrosis factor α increased significantly, which implied a greater inflammatory response in the fibrotic ALPPS group, especially in the early phase (Fig 3, *E*). Importantly, the significantly greater PT reflected poor coagulation function in the fibrotic ALPPS group ($P = .046$ on day 2). Moreover, unfavorable results, including a notably a lesser concentration of serum albumin and greater levels of ALT and total bilirubin (albeit nonsignificant changes), implied a more severe damage and inferior recovery in the ALPPS group for livers with fibrosis (Fig 3, *F*). To investigate functional proliferation, P450 enzymes, such as CYP1A1, CYP2A6, and CYP3A1, were measured by quantitative PCR with 3 biologic repetitions. The relatively lesser expression of CYP2A6 indicated that functional proliferation in ALPPS-derived new hepatocytes in livers with fibrosis lagged behind that in normal livers (Fig 3, *D*).

For stage II of the ALPPS procedure (Fig 4, A), 2 rats in the fibrotic ALPPS group ($n = 6$) died after the operation. The most likely reason was that of PHLF because of an insufficient FLR (Fig 4, *B*). The efficiency of ALPPS-induced proliferation after stage II was still inferior in livers with fibrosis ($P = .005$; Fig 4, *C*). Similarly, lesser levels of serum albumin in livers with fibrosis reflected more severe damage in ALPPS-derived stress ($P < .001$; Fig 4, *D*). Taken together, the data indicate that ALPPS-derived liver regeneration is feasible but attenuated in livers with fibrosis.

Discussion

Because majority of previous ALPPS cases were reported in normal livers, the data regarding the feasibility and safety of ALPPS in livers with fibrosis or cirrhosis remain poorly documented.[5,22] There is insufficient high-level evidence to support the feasibility of ALPPS in fibrotic livers because the compensatory proliferation after parenchymal damage is not well described. Experimental models are preferred because they are safer initially

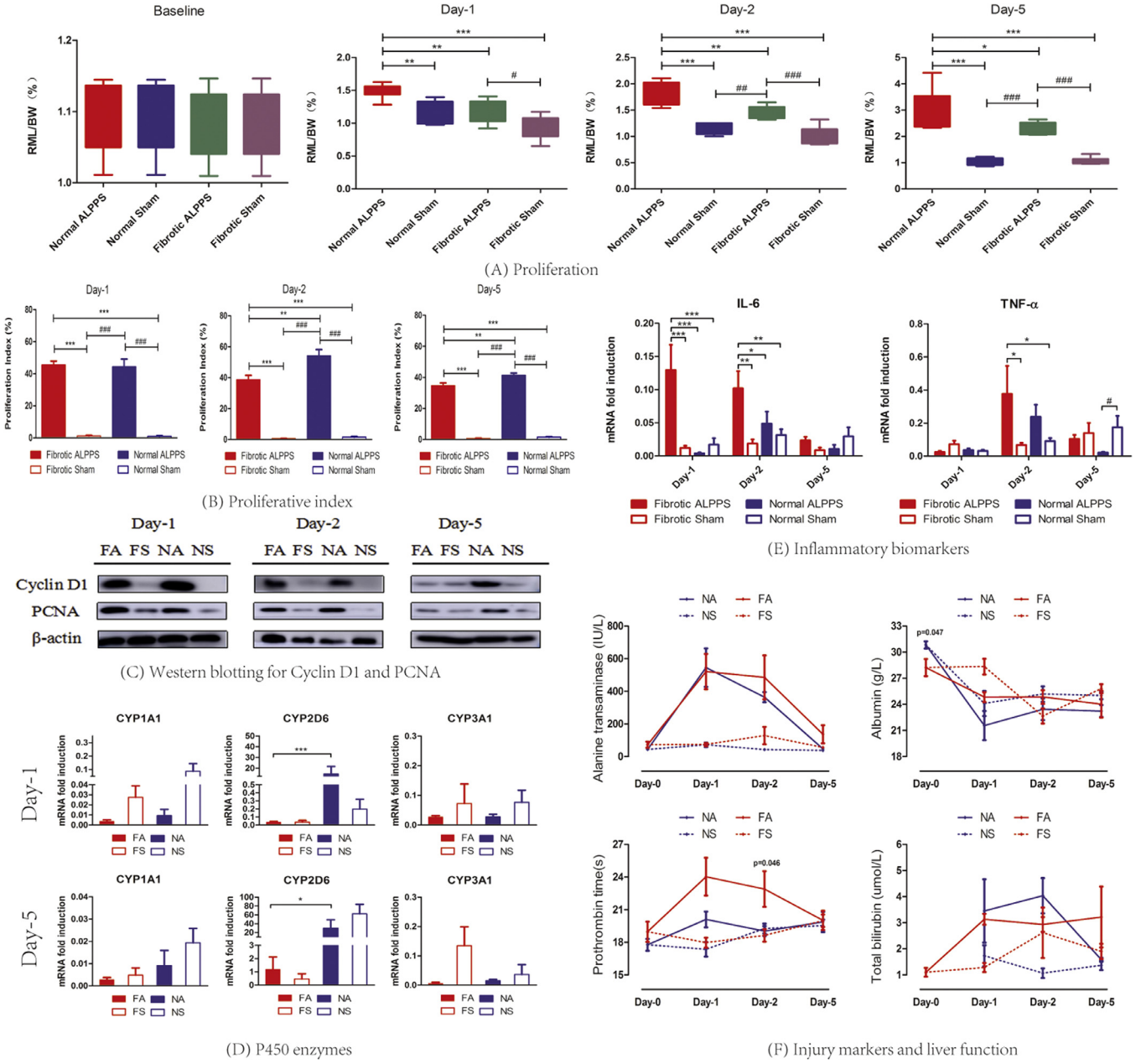

Fig. 3. Comparison of the different groups. (A) Comparison of the proliferation according to RML/BW induced by the ALPPS procedure in rat livers with or without fibrosis (n = 6 for each condition). (B) The proliferation indices were compared between the groups. (C) Western blot of PCNA and cyclin D1 for each group. (D) Relative mRNA expression of the P450 enzyme in the groups with three biological repetitions. (E) Inflammatory biomarkers in the groups with three biological repetitions. (F) Assessment of liver function in the groups. $^{*}P<0.05$, $^{**}P<0.01$, and $^{***}P<0.001$, represent the fibrotic ALPPS group compared with the other groups, while $^{\#}P<0.05$, $^{\#\#}P<0.01$, and $^{\#\#\#}P<0.001$ represent the normal ALPPS group compared with the other groups. FA, fibrotic ALPPS; FS, fibrotic sham; NA, normal ALPPS; NS, normal sham. RML, right middle lobe; BW, body weight, FLR, future liver remnant.

than studying humans, can be standardized to yield better reproducibility, summarize more powerful evidence, and achieve wider application, particularly for high-risk operations; thus we established an ALPPS model in rats with TAA-induced fibrosis to evaluate the feasibility of ALPPS in a fibrotic liver. Given its impressive capacity for promoting rapid FLR proliferation, ALPPS-derived regeneration in livers with fibrosis has important clinical implications.

To the best of our knowledge, this is the first animal model to evaluate the feasibility and function of the ALPPS procedure in livers with fibrosis. In this study the degree of fibrosis was relatively stable with the short interval time. Moreover, individual differences regarding the severity of fibrosis were negligible compared with normal livers. Overall, the establishment of this rat model of ALPPS in a fibrotic liver has yielded meaningful findings. Initially, compared with the ligation and sham groups in the fibrotic rat model, faster proliferation of the FLR suggests that ALPPS is feasible in rat livers with fibrosis. Another important finding is that the hypertrophy capacity in fibrotic livers deteriorated. As mentioned in a literature review reporting that regeneration has a negative linear correlation with the degrees of fibrosis, our previous study indicated that extreme insufficiency of the predicted FLR in livers with fibrosis prevented our ability to recommend the ALPPS procedure in such patients.[8] Given that long-term TAA treatment

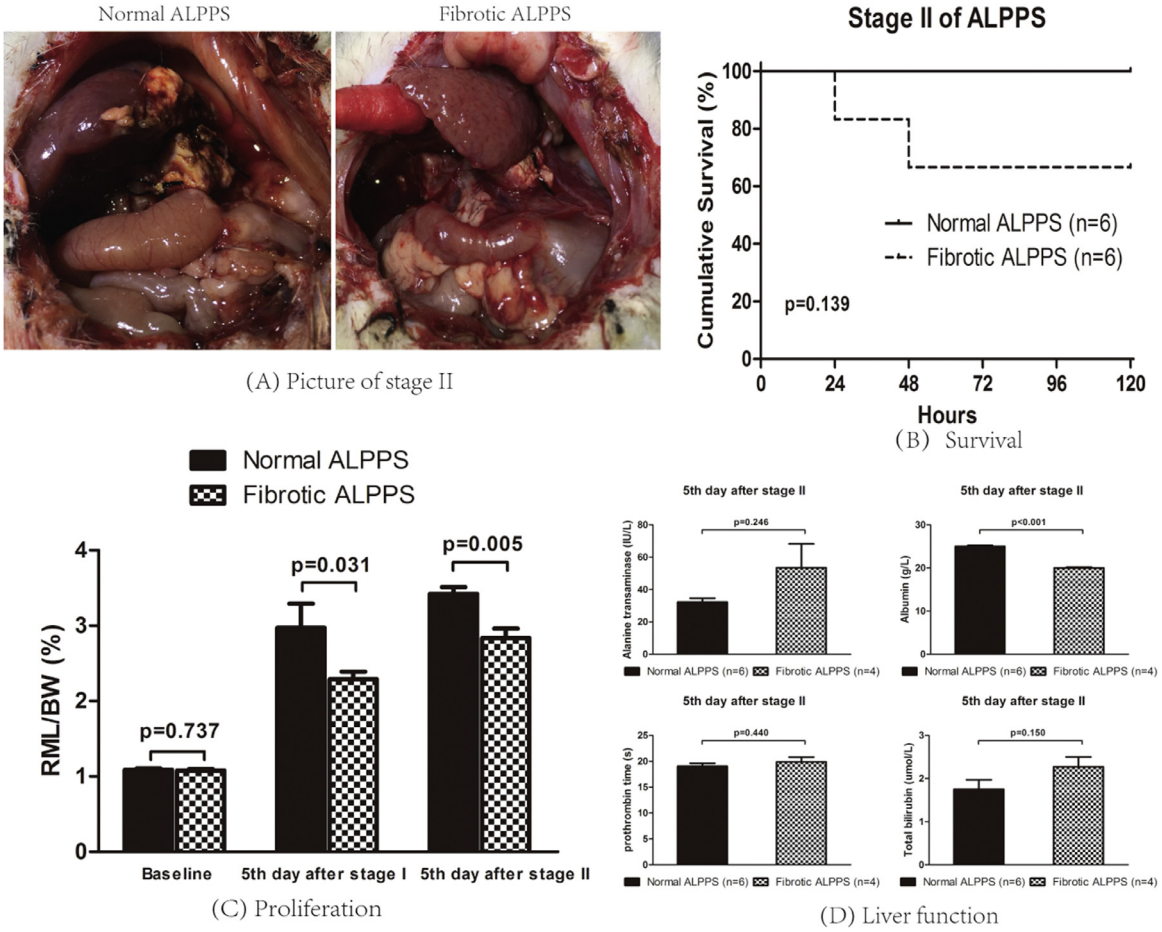

Fig. 4. Stage II of the ALPPS model in normal and fibrotic livers. (A) Image of stage II. (B) Survival after stage II of the ALPPS procedure (n = 6 for each condition). (C) Comparison of FLR regeneration in normal and fibrotic ALPPS groups. (D) Assessment of liver function after stage II. RML, right middle lobe; BW, body weight, FLR, future liver remnant.

leads to a broad range of fibrotic changes in the liver, the feasibility of ALPPS in mild or moderate fibrotic livers remains controversial. Negative correlations between the grade of fibrosis and liver regeneration after hepatectomy will be investigated in our follow-up study.

In clinical settings, because PHLF still occurs on occasion in patients with an otherwise adequate FLR as measured by the quantitative ratios of the FLR and the body weight, even with refinements in operative technique, doubts have been raised about the maturity and function of ALPPS-induced new hepatocytes, especially in diseased livers. The fate of cell development has been illustrated by lineage tracing methods, and basic studies have elucidated that it takes approximately 8 to 10 days for a hepatoblast to mature into a hepatocyte.[28,29] Within the short interval period of the ALPPS procedure, the origin of the induced hepatocytes is yet to be answered. Compared with the conventional partial hepatectomy model, which replenishes liver mass through the proliferation of mature hepatocyte,[28-30] our research indicates that hepatic progenitor cells might be activated by the ALPPS procedure to promote accelerated proliferation in the fibrotic liver of the rat.[26] In this study the lesser serum albumin levels, relatively downregulated CYP26D, and the 33% mortality in stage II in the fibrotic ALPPS group indicated that the process of new hepatocyte maturation and differentiation appears to be delayed. The first ALPPS consensus meeting held in Hamburg in 2015 indicated that stage II should be performed when the FLR reached 40% in livers with cirrhosis or 25% to 30% in normal livers.[31] Given the volumetrically and functionally impaired regenerative capacity in livers with fibrosis, the timing for stage II of ALPPS in livers with fibrosis should be evaluated with more caution, especially in patients with a marginally adequate FLR.

Although the hedgehog pathway has been involved in ALPPS-derived liver regeneration, additional mechanisms need to be evaluted.[21] Technically, FLR hypertrophy triggered by the ALPPS procedure may be related to the redistribution of portal inflow and the systemic inflammatory response.[10,17,18] Compared with conventional portal vein embolism, a greater regenerative response will be activated via complete devascularization between the hypertrophic and atrophic lobes, decreasing the microcirculation between the deportalized lobe and the FLR and accelerating FLR proliferation. After transection of the liver parenchyma, systemic increases in inflammatory factors promoting ALPPS-derived regeneration have been reported.[10] By using differential gene expression and enrichment of the KEGG pathways for ALPPS in normal and TAA-induced fibrotic livers via next generation sequencing, our future work will explore the specific molecular pathways mediating ALPPS-induced liver regeneration.

Several limitations should be acknowledged. First, the anatomic liver structure of rats is quite different from that of humans, so the rat model cannot completely mimic the clinical ALPPS procedure. Also, whether TAA-induced fibrosis can accurately represent other types of liver fibrosis or cirrhosis caused by, namely, viral hepati-

tis, alcohol abuse, nonalcoholic steatohepatitis, certain medications and hepatotoxins, and hereditary metabolic defects is controversial. The evidence to support the feasibility of ALPPS in such diseased livers is insufficient. Given the limitations of our rat model, several functional assessments of new hepatocytes, including hepatobiliary scintigraphy, indocyanine green clearance, and portal flow by Doppler measurements, are not easy to perform in this rat model. Therefore the maturity of ALPPS-induced regeneration in fibrotic livers needs to be elucidated fully in the future.

In conclusion, through the establishment of a rat model of TAA-induced fibrosis, we found that ALPPS-derived regeneration was feasible but attenuated in livers with fibrosis, which provided the preliminary theoretic foundation for the feasibility of ALPPS in fibrotic or cirrhotic livers.

Supplementary materials

Supplementary material associated with this article can be found, in the online version, at doi:10.1016/j.surg.2018.08.014.

References

1. Jackson R, Psarelli E, Berhane S, Khan H, Johnson P. Impact of viral status on survival in patients receiving sorafenib for advanced hepatocellular cancer: a meta-analysis of randomized phase III trials. *J Clin Oncol*. 2017;35:622–628.
2. Parkin DM, Bray F, Ferlay J, Pisani P. Estimating the world cancer burden: Globocan 2000. *Int J Cancer*. 2001;94:153–156.
3. Narita M, Oussoultzoglou E, Ikai I, Bachellier P, Jaeck D. Right portal vein ligation combined with in situ splitting induces rapid left lateral liver lobe hypertrophy enabling 2-staged extended right hepatic resection in small-for-size settings. *Ann Surg*. 2012;256:e7–e8.
4. de Santibañes E, Clavien PA. Playing Play-Doh to prevent postoperative liver failure. *Ann Surg*. 2012;255:415–417.
5. Schadde E, Ardiles V, Robles-Campos R, Malago M, Machado M, Hernandez-Alejandro R, et al. Early survival and safety of ALPPS: first report of the International ALPPS Registry. *Ann Surg*. 2014;260:829–836.
6. Seniutkin O, Furuya S, Luo YS, Cichocki JA, Fukushima H, Kato Y, et al. Effects of pirfenidone in acute and sub-chronic liver fibrosis, and an initiation-promotion cancer model in the mouse. *Toxicol Appl Pharmacol*. 2018;339:1–9.
7. Tiberio GA, Tiberio L, Benetti A, Cervi E, Montani N, Dreano M, et al. IL6 Promotes compensatory liver regeneration in cirrhotic rat after partial hepatectomy. *Cytokine*. 2008;42:372–378.
8. Cai X, Tong Y, Yu H, Liang X, Wang Y, Liang Y, et al. The ALPPS in the treatment of hepatitis B-related hepatocellular carcinoma with cirrhosis: a single-center study and literature review. *Surg Innov*. 2017;24:358–364.
9. Xiao L, Li JW, Zheng SG. Totally laparoscopic ALPPS in the treatment of cirrhotic hepatocellular carcinoma. *Surg Endosc*. 2015;29:2800–2801.
10. Schlegel A, Lesurtel M, Melloul E, Limani P, Tschuor C, Graf R, et al. ALPPS: from human to mice highlighting accelerated and novel mechanisms of liver regeneration. *Ann Surg*. 2014;260:839–846.
11. Almau Trenard HM, Moulin LE, Padín JM, Stringa P, Gondolesi GE, Barros Schelotto P. Development of an experimental model of portal vein ligation associated with parenchymal. *Cir Esp*. 2014;92:676–681.
12. Yao L, Li C, Ge X, Wang H, Xu K, Zhang A, et al. Establishment of a rat model of portal vein ligation combined with in situ splitting. *PLoS One*. 2014;9.
13. Croome KP, Mao SA, Glorioso JM, Krishna M, Nyberg SL, Nagorney DM. Characterization of a porcine model for associating liver partition and portal vein ligation for a staged hepatectomy. *HPB (Oxford)*. 2015;17:1130–1136.
14. Dhar DK, Mohammad GH, Vyas S, Broering DC, Malago M. A novel rat model of liver regeneration: possible role of cytokine induced neutrophil chemoattractant-1 in augmented liver regeneration. *Ann Surg Innov Res*. 2015;9:11.
15. García-Pérez R, Revilla-Nuin B, Martínez CM, Bernabé-García A, Baroja Mazo A, Parrilla Paricio P. Associated liver partition and portal vein ligation (ALPPS) vs selective portal vein ligation (PVL) for staged hepatectomy in a rat model. Similar regenerative response? *PLoS One*. 2015;10.
16. Shi H, Yang G, Zheng T, Wang J, Li L, Liang Y, et al. A preliminary study of ALPPS procedure in a rat model. *Sci Rep*. 2015;5:17567.
17. Wei W, Zhang T, Zafarnia S, Schenk A, Xie C, Kan C, et al. Establishment of a rat model: associating liver partition with portal vein ligation for staged hepatectomy. *Surgery*. 2016;159:1299–1307.
18. Liao M, Zhang T, Wang H, Liu Y, Lu M, Huang J, et al. Rabbit model provides new insights in liver regeneration after transection with portal vein ligation. *J Surg Res*. 2017;209:242–251.
19. Linecker M, Kambakamba P, Reiner CS, Linh Nguyen-Kim TD, Stavrou GA, Jenner RM, et al. How much liver needs to be transected in ALPPS? A translational study investigating the concept of less invasiveness. *Surgery*. 2017;161:453–464.
20. Langiewicz M, Schlegel A, Saponara E, Linecker M, Borger P, Graf R, et al. Hedgehog pathway mediates early acceleration of liver regeneration induced by a novel two-staged hepatectomy in mice. *J Hepatol*. 2017;66:560–570.
21. Andersen KJ, Knudsen AR, Jepsen BN, Meier M, Gunnarsson AP, Jensen UB, et al. A new technique for accelerated liver regeneration: an experimental study in rats. *Surgery*. 2017;162:233–247.
22. Sheng RF, Wang HQ, Jin KP, Yang L, Liu H, Ji Y, et al. Histogram analyses of diffusion kurtosis indices and apparent diffusion coefficient in assessing liver regeneration after ALPPS and a comparative study with portal vein ligation. *J Magn Reson Imaging*. 2018;47:729–736.
23. Deal R, Frederiks C, Williams L, Olthof PB, Dirscherl K, Keutgen X, et al. Rapid liver hypertrophy after portal vein occlusion correlates with the degree of collateralization between lobes-a study in pigs. *J Gastrointest Surg*. 2018;22:203–213.
24. An SY, Jang YJ, Lim HJ, Han J, Lee J, Lee G, et al. Milk fat globule-EGF factor 8, secreted by mesenchymal stem cells, protects against liver fibrosis in mice. *Gastroenterology*. 2017;152:1174–1186.
25. Karp NA, Meehan TF, Morgan H, Mason JC, Blake A, Kurbatova N, et al. Applying the ARRIVE guidelines to an in vivo database. *PLoS Biol*. 2015;13.
26. Ishak K, Baptista A, Bianchi L, Callea F, De Groote J, Gudat F, et al. Histological grading and staging of chronic hepatitis. *J Hepatol*. 1995;22:696–699.
27. Tong YF, Meng N, Chen MQ, Ying HN, Xu M, Lu B, et al. Maturity of associating liver partition and portal vein ligation for staged hepatectomy-derived liver regeneration in a rat model. *World J Gastroenterol*. 2018;24:1107–1119.
28. Font-Burgada J, Shalapour S, Ramaswamy S, Hsueh B, Rossell D, Umemura A, et al. Hybrid periportal hepatocytes regenerate the injured liver without giving rise to cancer. *Cell*. 2015;162:766–779.
29. Song G, Pacher M, Balakrishnan A, Yuan Q, Tsay HC, Yang D, et al. Direct reprogramming of hepatic myofibroblasts into hepatocytes in vivo attenuates liver fibrosis. *Cell Stem Cell*. 2016;18:797–808.
30. Michalopoulos GK. Hepatostat: liver regeneration and normal liver tissue maintenance. *Hepatology*. 2017;65:1384–1392.
31. Oldhafer KJ, Stavrou GA, van Gulik TMCore Group. ALPPS—where do we stand, where do we go? Eight recommendations from the first international expert meeting. *Ann Surg*. 2016;263:839–841.